Research Article Vol. 31, No. 10 / 8 May 2023 / Optics Express 15326

Optics EXPRESS

980 nm electrically pumped continuous lasing of QW lasers grown on silicon

Qi Lin,[1,†] Jie Huang,[1,†] Liying Lin,[1] Wei Luo,[1] Wen Gu,[1] and Kei May Lau[1,2,3,*]

[1] *Department of Electronic and Computer Engineering, Hong Kong University of Science and Technology, Clear Water Bay, Kowloon, Hong Kong*
[2] *Department of Electronic Engineering, Chinese University of Hong Kong, Shatin, N.T., Hong Kong*
[3] *kmlau@ee.cuhk.edu.hk*
[†] These authors contributed equally to this work
[*] *eekmlau@ust.hk*

Abstract: Investigation of high-performance lasers monolithically grown on silicon (Si) could promote the development of silicon photonics in regimes other than the 1.3 -1.5 µm band. 980 nm laser, a widely used pumping source for erbium-doped fiber amplifier (EDFA) in the optical fiber communication system, can be used as a demonstration for shorter wavelength lasers. Here, we report continuous wave (CW) lasing of 980 nm electrically pumped quantum well (QW) lasers directly grown on Si by metalorganic chemical vapor deposition (MOCVD). Utilizing the strain compensated InGaAs/GaAs/GaAsP QW structure as the active medium, the lowest threshold current obtained from the lasers on Si was 40 mA, and the highest total output power was near 100 mW. A statistical comparison of lasers grown on native GaAs and Si substrates was conducted and it reveals a somewhat higher threshold for devices on Si. Internal parameters, including modal gain and optical loss are extracted from experimental results and the variation on different substrates could provide a direction to further laser optimization through further improvement of the GaAs/Si templates and QW design. These results demonstrate a promising step towards optoelectronic integration of QW lasers on Si.

1. Introduction

Si photonics is booming for data processing and optical communication, owing to its high-speed performance, potential low-cost, high-volume manufacturing capabilities and compatibility with the CMOS technology [1]. The Si platform has witnessed remarkable advancement in the integration of waveguides [2], modulators [3], and photodetectors [4]. From a long-term perspective, heterogeneous epitaxy of lasers on Si could achieve high yield and scalability, compared with the commonly used bonding technique. Due to the direct bandgap structure of III-V alloys, III-V based electro-optical devices on Si have showed good performance. However, the laser sources grown on Si always suffer from performance degradation due to high-density of defects caused by the large lattice mismatch between III-V alloys and Si [5,6]. To mitigate this issue, the growth of high-quality GaAs/Si templates have incorporated strained layer superlattices (SLSs) [7], thermal cycle annealing (TCA) [8] and compositionally graded buffer [9]. In addition, it has been reported that quantum well (QW) [10,11] could be utilized in the active region grown on Si with high efficiency and thus promoting device performance.

To date, the remarkable lasers emitting at 1.3-1.5 µm band have been successfully achieved on Si by MOCVD [12–14]. However, the demand for information interaction still requires a reliable 980 nm laser source for EDFAs, to achieve higher pumping efficiency and lower amplifier noise [15]. InGaAs/GaAs QW lasers emitting in the 880–1100 nm wavelength regime can be achieved by changing the indium concentration or thickness of InGaAs QW [16], and excellent device performance has been demonstrated on the native GaAs substrates [17,18]. However, a

#484831 https://doi.org/10.1364/OE.484831
Journal © 2023 Received 4 Jan 2023; revised 17 Feb 2023; accepted 21 Feb 2023; published 24 Apr 2023

high indium concentration for enhanced optical efficiency could induce severe lattice mismatch between InGaAs and GaAs, and hence generate defects, which degrades laser internal quantum efficiency [19,20]. Utilizing InGaAs/AlGaAs QW as an alternative, C. Jiang et al. recently demonstrated an electrically pumped 980 nm laser grown on Si by molecular beam epitaxy (MBE) with a low threshold current in CW mode. But the lifetime of the laser is unacceptably short at room temperature [21]. Yet, the high temperature required for the AlGaAs barrier growth would cause the segregation of Indium atoms in the InGaAs layer growth [22]. Besides, the interfacial oxygen generated in the AlGaAs growth could also degrade the quality of the InGaAs/AlGaAs QW [23], leading to a dramatic decrease in the recombination lifetime of carriers [24]. Alternatively, the strain-compensated InGaAs/GaAs/GaAsP QW structure could provide enhanced carrier confinement and strain compensation, leading to a lower laser threshold and better temperature stability [25,26]. Here, we report continuous-wave (CW) lasing of 980 nm QW lasers, combining the advantages of InGaAs/GaAs/GaAsP QW with high-quality GaAs/Si templates. The lowest threshold measured on devices with 2 μm × 1 mm cavity was 40 mA. The lowest threshold density is 937.5 A/cm^2 obtained on devices with 40 μm × 1.2 mm cavity. The total output power is nearly 100 mW, and the highest operating temperature is above 95 °C which is limited by the setup.

2. Experiment

The electrically pumped InGaAs/GaAs/GaAsP QW lasers were grown on CMOS-compatible nominal (001) Si by MOCVD and the schematic diagram of the laser structure is delineated in Fig. 1(a). The GaAs/Si templates and the laser structure were grown in an AIXTRON CCS system, and AIXTRON 200/4 system, respectively. The growth of GaAs on Si began with the deposition of 1 μm-thick GaAs with the temperature changing from 400 °C to 560 °C, and two sets of TCA were performed on the GaAs/Si templates between 730 °C and 330 °C, to improve the quality of GaAs film. After that, one set of ten periods of 9.5 nm $In_{0.15}GaAs$/12 nm GaAs strained-layer super-lattices (SLSs) was inserted in the GaAs to filter the threading dislocations densities (TDDs). The total thickness of the GaAs buffer with SLSs is 2 μm, and the defect density of the GaAs/Si templates obtained from statistical data over an area of 200 μm^2 (measured by plan-view transmission electron microscopy (PV-TEM)), is counted to be 2.8×10^7 /cm^2, as shown in Fig. 1(b).

A 700 nm n-type GaAs contact layer and an 800 nm n-type $Al_{0.7}GaAs$ cladding were sequentially grown on the GaAs/Si templates and GaAs substrate. Strain-compensated InGaAs/GaAs/GaAsP QW structure was then grown as the active region. An 800 nm $Al_{0.7}GaAs$ p-cladding layer, and a 200 nm p-type GaAs contact layer were finally grown with detailed parameters reported in Ref. [27]. Figure 1(b) shows the cross-sectional TEM image of the laser structure grown on Si. The room temperature (RT) μPL spectra of the InGaAs/GaAs/GaAsP QWs on GaAs and GaAs/Si template without cladding and contact layer, excited by a CW 514 nm laser under the same power, is shown in Fig. 1(d). A similar peak wavelength of 956 nm was observed on both GaAs and Si substrates. The 10 × 10 μm^2 AFM image of the electrically pumped InGaAs/GaAs/GaAsP QW laser grown on Si is shown in Fig. 1(e). The measured surface roughness of 2.1 nm is sufficiently smooth for the subsequent device fabrication.

The as-grown samples were fabricated into ridge waveguide edge-emitting lasers to investigate the device performance of the InGaAs/GaAs/GaAsP QWs lasers, as shown in Fig. 2(a). The lasers were defined by conventional photolithography and dry etching steps. Ti/Pt/Au and Ge/Au/Ni/Au were deposited as *P* and *N* metals, respectively. After 600 nm SiO_2 passivation and metal pad deposition, the samples were thinned down to 100 μm and cleaved to various-lengths laser bars with uncoated facets. The 52°-titled SEM image of a ridge waveguide laser with a first mesa width of 6 μm, is shown in Fig. 2(b), illustrating vertical and smooth sidewalls for good optical confinement.

Optics EXPRESS

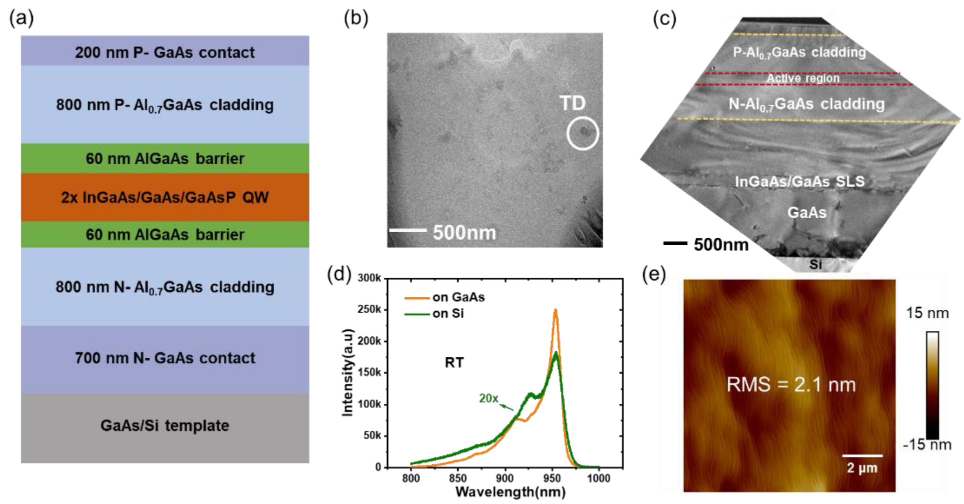

Fig. 1. (a) Schematic of the 980 nm InGaAs/GaAs/GaAsP QW laser grown on GaAs/Si template; (b) PV-TEM images of 2 μm-thick GaAs/Si template; (c) Global view cross-sectional TEM image of the laser structure grown on Si; (d) Room temperature (RT) μPL of the InGaAs/GaAs/GaAsP QW grown on GaAs and Si; (e) AFM images of the electrically pumped InGaAs/GaAs/GaAsP QW laser grown on Si. The color scale of the AFM image is 30 nm.

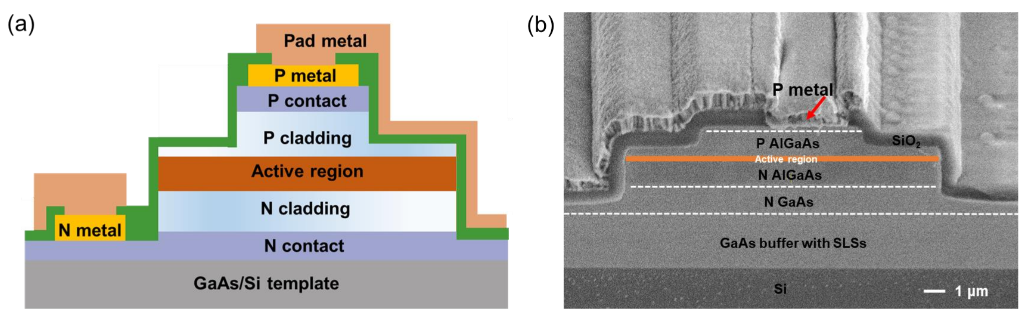

Fig. 2. (a) Schematic cross-section of the fabricated device on Si. (b) SEM images of the end-facet of ridge waveguide laser grown on Si.

3. Result and discussion

The fabricated lasers were placed on a heatsink with a temperature controller and electrically driven by a current source in CW mode. The lowest threshold current is 40 mA, obtained on the 2 μm × 1 mm device. Figure 3(a), the light-current (L-I) curve of a representative InGaAs/GaAs/GaAsP QW laser grown on Si, with cavity size of 4 μm × 1 mm, exhibits a low threshold current of ~80 mA and high output power more than 30 mW. The current-voltage (I-V) characteristics (inset of Fig. 3(a)) shows a turn-on voltage of 1.1 V and a resistance of 9.1 Ω. The RT emission spectra with intensity in log scale of the corresponding 4 μm × 1 mm device with increasing current injection, as shown in Fig. 3(b), were observed from an optical spectrum analyzer by coupling the output light from the end facet into a lensed fiber. A distinct peak at 983 nm is observed at 70 mA (0.88 I_{th}), and the distinction ratio under 110 mA (1.38 I_{th}) was above 21 dB. With a narrow ridge of 4 µm, single-mode lasing was achieved at a certain current injection range.

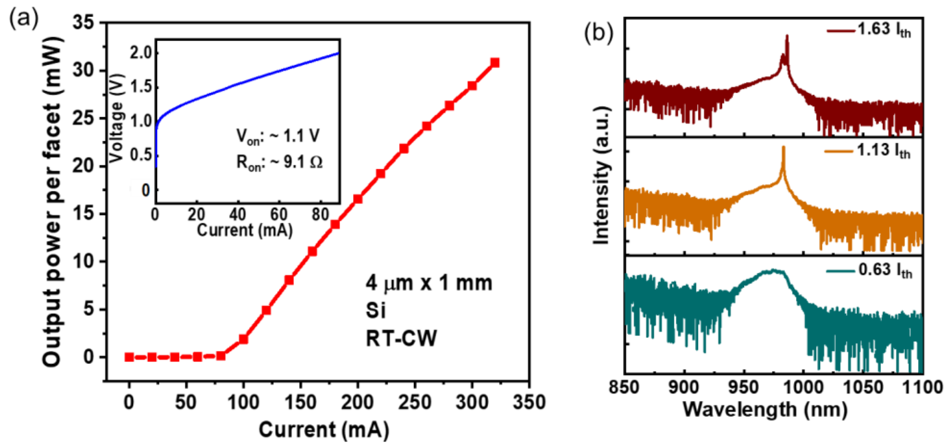

Fig. 3. (a) Representative L-I curves of the laser grown on Si; Inset: I-V curves of the laser; (b) Emission spectra at progressively increased currents of the 4 µm × 1 mm laser grown on the Si measured at 20 °C in CW mode.

To compare the optical performance of lasers grown on GaAs and Si substrates, a statistical analysis was performed with more than 30 devices measured on each substrate. The light-current (L-I) curves and the distribution of threshold current density of InGaAs/GaAs/GaAsP QW lasers with different dimensions on GaAs and Si are shown in Fig. 4(a)-(b). The single-facet output power of lasers is 65 mW on native GaAs, and is 46.4 mW on Si, without obvious saturation or degradation. The net gain of those devices with larger cavity size is higher and thus the threshold current density is smaller [28]. The lowest threshold current density of lasers achieved on GaAs is 179 A/cm^2, obtained on an 70 µm × 2 mm device, and on Si is 938 A/cm^2 on an 40 µm × 1.2 mm device. The thresholds of lasers grown on GaAs congregate well while those grown on Si show a larger variation. The difference in the threshold distribution between GaAs and Si could be attributed to the uniformity of grown QW and the quality of GaAs/Si templates. Initial results show that the average threshold current density of the ridge waveguide lasers on Si (~1.91 kA/cm^2), is approximately five times higher than devices on the native GaAs substrate (~ 410 A/cm^2).

For a detailed analysis and comparison, cavity length-dependent measurements were performed to extract the internal parameters of InGaAs/GaAs/GaAsP QW lasers, including the internal quantum efficiency (IQE) η_i, internal loss α_i, modal gain Γg_0 and transparency current density J_{tr}. The differential quantum efficiency (DQE) was first calculated from the slope of each L-I curve of lasers with the same cavity width based on the formula: $\eta_d = \frac{q}{h\nu} \cdot \frac{dP_0}{dI}$, where q is the electron charge, h is the Planck's constant, ν corresponds to the lasing frequency, P_0 is the total output power and I is the injection current. As shown in Fig. 4(c)-(d), the reciprocal of η_d as a function of cavity length was plotted, and then fitted with the equation $\frac{1}{\eta_d} = \frac{L \cdot \alpha_i}{\eta_i \cdot ln\left(\frac{1}{R}\right)} + \frac{1}{\eta_i}$, where R is the mean mirror reflectivity, around 0.3 normally for GaAs-based cleaved mirrors [29]. $\eta_i = 46.4\%$, $\alpha_i = 9.6\,\mathrm{cm}^{-1}$ and $\eta_i = 28.5\%$, $\alpha_i = 32.7\,\mathrm{cm}^{-1}$ were extracted for lasers on GaAs and Si, respectively. The relationship of threshold current density and cavity length satisfies the formula $J_{th} = J_{tr} \cdot e^{\frac{\alpha_i + \frac{1}{L} \cdot ln\left(\frac{1}{R}\right)}{\Gamma g_0}}$. Fitting the experimental data, shown in Figs. 4(e)-(f), the transparency current density J_{tr} and the modal gain Γg_0 can be extrapolated to be $\Gamma g_0 = 27.4\,\mathrm{cm}^{-1}$, $J_{tr} = 330$ A/cm^2 on GaAs and $\Gamma g_0 = 23.7\,\mathrm{cm}^{-1}$, $J_{tr} = 370$ A/cm^2 on Si. The lower modal gain

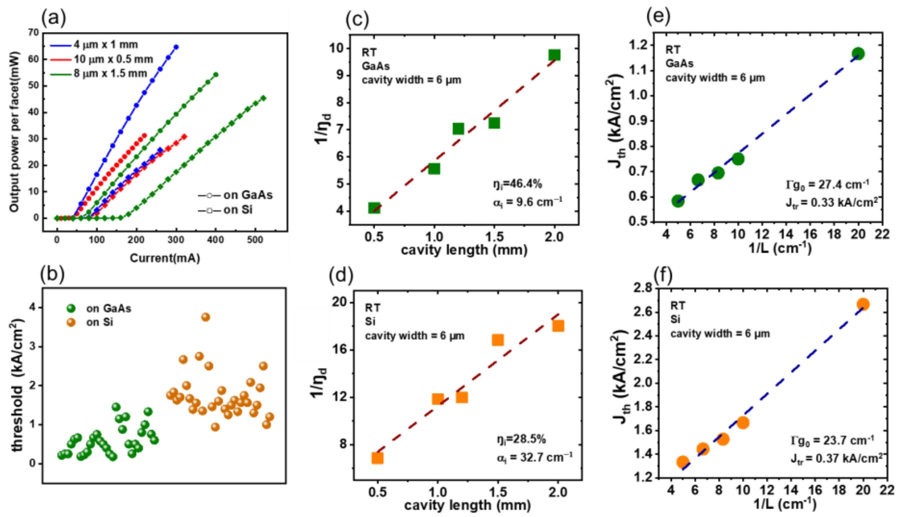

Fig. 4. (a) L-I curves of InGaAs/GaAs/GaAsP QW lasers with various cavity size grown on GaAs and Si; (b) Threshold density distribution on GaAs and Si; (c) (d) Extraction of the internal quantum efficiency (IQE η_i), internal loss (α_i), (e) (f) model gain (Γg_0) and transparency current density (J_{tr}), from cavity length dependent measurement on GaAs and Si.

and IQE for QW grown on Si are consistent with the higher experimental threshold of lasers on Si, primarily arising from the more non-radiative recombination induced by defects in the active region grown on Si. Based on the investigation of the internal parameters, a better laser performance with lower non-radiative losses can be achieved by further reducing the defects density of the GaAs film grown on Si substrate via additional dislocation reduction approaches [30]. In addition, laser performance improvement could also be achieved by enhancing the quality of QWs through optimization of parameters including the QW thickness and indium composition [31].

For practical application, the temperature stability of lasers in CW mode is of great importance. Temperature-dependent L-I measurements were performed to examine the high-temperature operation of lasers on different substrates. Figure 5(a)-(b) present the L-I characteristics of the 4 μm × 1.5 mm lasers on GaAs and Si at various heat sink temperatures. The lasers grown on both GaAs and Si substrates can lase above 95 °C, which is the limitation of the measurement setup. At elevated temperatures, the threshold current increases but no significant decrease of slope efficiency was observed, as shown in the insets of Fig. 5(a)-(b). Using $\frac{I_{th}(T_2)}{I_{th}(T_1)} = exp\left(\frac{T_2-T_1}{T_0}\right)$, the characteristic temperature of $T_0 = 139.1$ K and $T_0 = 71.8$ K can be extracted for the lasers grown on GaAs and Si, respectively. The highest characteristic temperature obtained on GaAs and Si is 157 K (10 μm × 0.5 mm) and 84 K (2 μm × 1.5 mm), as presented in Fig. 5(c)-(d). The characteristic temperatures of lasers on Si are somewhat lower than those on native GaAs substrate, suggesting inferior temperature stability of defect-limited threshold current. Compared with the reported room-temperature operation lasers on Si [32,33], the high-temperature operation here proves outstanding temperature stability of the InGaAs/GaAs/GaAsP QW structure.

Optics EXPRESS

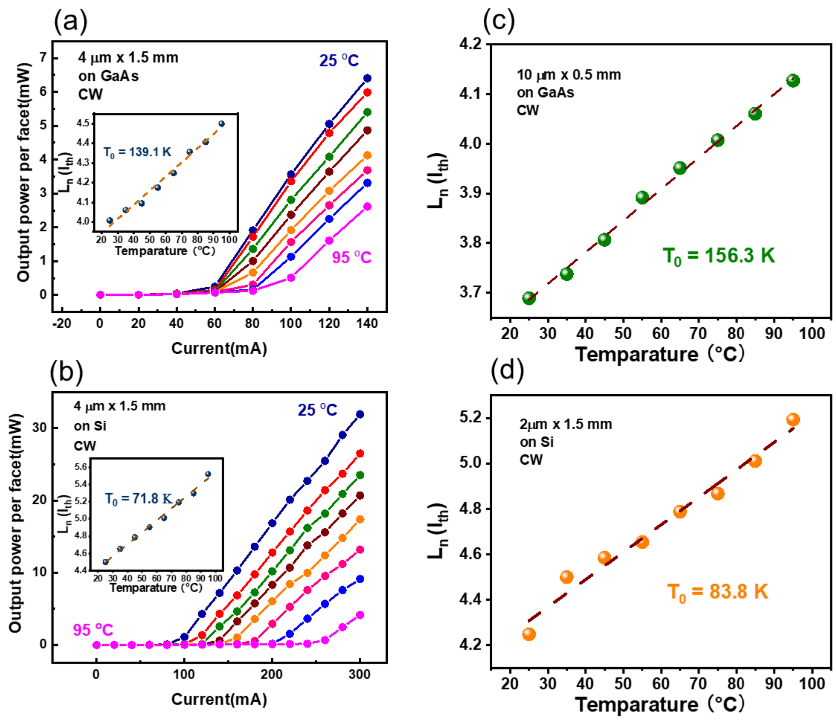

Fig. 5. Temperature-dependent L-I curves of the 4 μm × 1.5 mm lasers grown on (a) GaAs and (b) Si substrate, respectively; Highest characteristic temperature of InGaAs/GaAs/GaAsP QW lasers grown on (c) GaAs and (d) Si substrate, respectively.

4. Conclusion

In conclusion, we compared characteristics of electrically pumped CW lasing InGaAs/GaAs/GaAsP QW lasers monolithically grown on (001) Si emitting at 980 nm with those on GaAs native substrates. The strain-compensated InGaAs/GaAs/GaAsP QWs provide an efficient and reliable active region in laser structure with emission wavelength at ~980 nm on Si. The GaAs/Si template with a low defect density used in the full laser structure also contributes to a respectable laser performance, with the lowest laser threshold density of 938 A/cm^2, highest total output power of 97 mW, a high operating temperature above 95 °C with a high characteristic temperature under CW mode. Detailed investigation of internal parameters from the experiment facilitates the material evaluation and feedback optimization. All these results are important steps forward the heterogeneous epitaxy of III-V light sources for Si photonics and guide the further optimization of high-performance 980 nm QW lasers. The demonstration paves the way toward the integration with Si photonics for a variety of applications including optical fiber communication and internet protocol networks.

Funding. University Grants Committee (16213420); Innovation and Technology Fund (ITS/201/19FP).

Acknowledgments. The authors would like to thank Nanosystem Fabrication Facility (NFF) and the Material Characterization & Preparation Facility (MCPF) of HKUST for their technical support.

Disclosures. The authors declare no conflicts of interest.

Data availability. Data underlying the results presented in this paper are not publicly available at this time but may be obtained from the authors upon reasonable request.

References

1. D. Thomson, A. Zilkie, J. E. Bowers, T. Komljenovic, G. T. Reed, L. Vivien, D. Marris-Morini, E. Cassan, L. Virot, and J.-M. Fédéli, "Roadmap on silicon photonics," J. Opt. **18**(7), 073003 (2016).
2. N. Kazanskiy, M. Butt, and S. Khonina, "Silicon photonic devices realized on refractive index engineered subwavelength grating waveguides-a review," Opt. Laser Technol. **138**, 106863 (2021).
3. R. Amin, R. Maiti, Y. Gui, C. Suer, M. Miscuglio, E. Heidari, R. T. Chen, H. Dalir, and V. J. Sorger, "Sub-wavelength Ghz-fast broadband ITO mach–zehnder modulator on silicon photonics," Optica **7**(4), 333–335 (2020).
4. Y. Xue, Y. Wang, W. Luo, J. Huang, L. Lin, H. K. Tsang, and K. M. Lau, "Telecom InP-based quantum dash photodetectors grown on Si," Appl. Phys. Lett. **118**(14), 141101 (2021).
5. D. Liang and J. E. Bowers, "Recent progress in lasers on silicon," Nat. Photonics **4**(8), 511–517 (2010).
6. Y. Wan, C. Xiang, J. Guo, R. Koscica, M. Kennedy, J. Selvidge, Z. Zhang, L. Chang, W. Xie, D. Huang, A. C. Gossard, and J. E. Bowers, "High speed evanescent quantum-dot lasers on Si," Laser Photonics Rev. **15**, 2100057 (2021).
7. Y. Takano, M. Hisaka, N. Fujii, K. Suzuki, K. Kuwahara, and S. Fuke, "Reduction of threading dislocations by InGaAs interlayer in GaAs layers grown on Si substrates," Appl. Phys. Lett. **73**(20), 2917–2919 (1998).
8. Y. Ababou, P. Desjardins, A. Chennouf, R. Leonelli, D. Hetherington, A. Yelon, G. L'Espérance, and R. Masut, "Structural and optical characterization of InP grown on Si (111) by metalorganic vapor phase epitaxy using thermal cycle growth," J. Appl. Phys. (Melville, NY, U. S.) **80**(9), 4997–5005 (1996).
9. B. Shi and J. Klamkin, "Defect engineering for high quality InP epitaxially grown on on-axis (001) Si," J. Appl. Phys. (Melville, NY, U. S.) **127**(3), 033102 (2020).
10. L. Megalini, B. Bonef, B. C. Cabinian, H. Zhao, A. Taylor, J. S. Speck, J. E. Bowers, and J. Klamkin, "1550-nm InGaAsP multi-quantum-well structures selectively grown on V-groove-patterned SOI substrates," Appl. Phys. Lett. **111**(3), 032105 (2017).
11. J. Margetis, Y. Zhou, W. Dou, P. C. Grant, B. Alharthi, W. Du, A. Wadsworth, Q. Guo, H. Tran, S. Ojo, and G. Abernathy, "All group-IV SiGeSn/GeSn/SiGeSn QW laser on Si operating up to 90 K," Appl. Phys. Lett. **113**(22), 221104 (2018).
12. M. Buffolo, L. Rovere, C. De Santi, D. Jung, J. Norman, J. E. Bowers, R. W. Herrick, G. Meneghesso, E. Zanoni, and M. Meneghini, "Degradation of 1.3 µm InAs quantum-dot laser diodes: Impact of dislocation density and number of quantum dot layers," IEEE J. Quantum Electron. **57**(1), 1–8 (2021).
13. J. Wang, Z. Liu, H. Liu, Y. Bai, B. Ma, C. Xiao, C. Jiang, J. Li, H. Wang, Y. Jia, and X. Ren, "High slope-efficiency quantum-dot lasers grown on planar exact silicon (001) with asymmetric waveguide structures," Opt. Express **30**(7), 11563–11571 (2022).
14. L. Lin, Y. Xue, J. Li, W. Luo, J. Huang, and K. M. Lau, "C and L band room-temperature continuous-wave InP-based microdisk lasers grown on silicon," Opt. Lett. **46**(12), 2836–2839 (2021).
15. J. H. Lee, W. J. Lee, and N. Park, "Comparative study on temperature-dependent multichannel gain and noise figure distortion for 1.48-and 0.98-µm pumped EDFAs," IEEE Photonics Technol. Lett. **10**(12), 1721–1723 (1998).
16. G. Ji, D. Huang, U. Reddy, T. Henderson, R. Houdre, and H. Morkoc, "Optical investigation of highly strained InGaAs-GaAs multiple quantum wells," J. Appl. Phys. (Melville, NY, U. S.) **62**(8), 3366–3373 (1987).
17. K. Hsu, C. Ho, Y. Lin, Y. Wu, R. Hsu, and K. Huang, "Optical and electrical characteristics of GaAs/InGaAs quantum-well device," J. Alloys Compd. **471**(1-2), 567–569 (2009).
18. M. Bugajski, B. Mroziewicz, K. Regiński, J. Muszalski, K. Kosiel, M. Zbroszczyk, T. Ochalski, T. Piwoński, D. Wawer, A. Szerling, and E. Kowalczyk, "High power QW SCH InGaAs/GaAs lasers for 980-nm band," Bull. Pol. Acad. Sci. Tech.206Sci 53, (2005).
19. E. Zielińska-Rohozińska, J. Gronkowski, K. Pakuła, M. Majer, M. Regulska, and L. Nowicki, "Strain relaxation in $Ga_{1-x}In_xN$ thin layers grown on GaN sublayers," J. Alloys Compd. **328**(1-2), 199–205 (2001).
20. J. Sass, K. Mazur, F. Eichhorn, W. Strupiński, A. Turos, and N. Schell, "Determination of In concentration in InGaAs/GaAs 001 epilayers in the early stage of anisotropic stress relaxation," J. Alloys Compd. **401**(1-2), 249–253 (2005).
21. C. Jiang, H. Liu, J. Wang, X. Ren, Q. Wang, Z. Liu, B. Ma, K. Liu, R. Ren, Y. Zhang, S. Cai, and Y. Huang, "Demonstration of room-temperature continuous-wave operation of InGaAs/AlGaAs quantum well lasers directly grown on on-axis silicon (001)," Appl. Phys. Lett. **121**(6), 061102 (2022).
22. A. Marmalyuk, O. Govorkov, A. Petrovsky, D. Nikitin, A. Padalitsa, P. Bulaev, I. Budkin, and I. Zalevsky, "Investigation of indium segregation in InGaAs/(Al) GaAs quantum wells grown by MOCVD," J. Cryst. Growth **237-239**, 264–268 (2002).

Optics EXPRESS

23. R. N. Bicknell-Tassius, K. Lee, A. S. Brown, G. Dagnall, and G. May, "The growth of AlGaAs-InGaAs quantum-well structures by molecular beam epitaxy: Observation of critical interdependent effects," Appl. Phys. Lett. **70**(1), 52–54 (1997).
24. J. Orton, P. Dawson, D. Lacklison, T. Cheng, and C. Foxon, "Recombination lifetime measurements in AlGaAs/GaAs quantum well structures," Semicond. Sci. Technol. **9**(9), 1616–1622 (1994).
25. C. Chen, P. O. Leisher, A. A. Allerman, K. M. Geib, and K. D. Choquette, "Temperature analysis of threshold current in infrared vertical-cavity surface-emitting lasers," IEEE J. Quantum Electron. **42**(10), 1078–1083 (2006).
26. K. Bacher, S. Massie, and M. Seaford, "Molecular beam epitaxy of strain-compensated InGaAs/GaAsP quantum-well intersubband photodetectors," J. Cryst. Growth **175-176**, 977–982 (1997).
27. W. Luo, L. Lin, J. Huang, Q. Lin, and K. M. Lau, "Electrically pumped InP/GaAsP quantum dot lasers grown on (001) Si emitting at 750 nm," Opt. Express **30**(22), 40750–40755 (2022).
28. L. Asryan and R. Suris, "Inhomogeneous line broadening and the threshold current density of a semiconductor quantum dot laser," Semicond. Sci. Technol. **11**(4), 554–567 (1996).
29. S. W. Koch and M. R. Hofmann, "Semiconductor lasers," in *Encyclopedia of Modern Optics* (Second Edition), B. D. Guenther and D. G. Steel, eds. (Elsevier, Oxford, 2018), pp. 462–468, second edition ed.
30. C. Shang, J. Selvidge, E. Hughes, J. C. Norman, A. A. Taylor, A. C. Gossard, K. Mukherjee, and J. E. Bowers, "A pathway to thin GaAs virtual substrate on on-axis Si (001) with ultralow threading dislocation density," Phys. Status Solidi A **218**(3), 2000402 (2021).
31. A. Kasukawa, R. Bhat, C. Zah, M. Koza, and T. Lee, "Very low threshold current density 1.5 µm GaInAs/AlGaInAs graded-index separate-confinement-heterostructure strained quantum well laser diodes grown by organometallic chemical vapor deposition," Appl. Phys. Lett. **59**(20), 2486–2488 (1991).
32. X. Huang, Y. Song, T. Masuda, D. Jung, and M. Lee, "InGaAs/GaAs quantum well lasers grown on exact GaP/Si (001)," Electron Lett. **50**(17), 1226–1227 (2014).
33. V. Y. Aleshkin, N. Baidus, A. Dubinov, A. Fefelov, Z. Krasilnik, K. Kudryavtsev, S. Nekorkin, A. Novikov, D. Pavlov, I. Samartsev, and E. Skorokhodov, "Monolithically integrated InGaAs/GaAs/AlGaAs quantum well laser grown by MOCVD on exact Ge/Si (001) substrate," Appl. Phys. Lett. **109**(6), 061111 (2016).